energies

MDPI

Article

Study of a Combined Demagnetization and Eccentricity Fault in an AFPM Synchronous Generator

Alexandra C. Barmpatza * and Joya C. Kappatou

Department of Electrical and Computer Engineering, University of Patras, 26504 Patras, Greece; joya@ece.upatras.gr

* Correspondence: abarmpatza@upatras.gr; Tel.: +30-694-2479943

Received: 22 September 2020; Accepted: 26 October 2020; Published: 27 October 2020

Abstract: This article investigates the combined partial demagnetization and static eccentricity fault in an Axial Flux Permanent Magnet (AFPM) Synchronous Generator. The machine is simulated using 3D FEM, while the EMF spectrum is analyzed in order to export the fault related harmonics using the FFT analysis. Firstly, the partial demagnetization fault, without the coexistence of eccentricity, and both the static angular and axis eccentricity faults, without the coexistence of partial demagnetization, are studied. In the case of eccentricity fault, the phase EMF sum spectrum has also been used as a diagnostic mean, because, when only eccentricity fault exists in the generator (either angular or axis) new harmonics do not appear in the EMF spectrum. Secondly the combination of partial demagnetization fault with static axis and static angular eccentricity is investigated and different comparisons are made when the demagnetization and the eccentricity level changes. The investigation revealed that the combination of eccentricity and demagnetization creates new harmonics in the EMF spectrum. The novelty of the article is that these combined faults are studied for the first time in the international literature, and the phase EMF sum spectrum has not been previously used for eccentricity diagnosis in this machine type.

Keywords: axial flux; demagnetization; finite element analysis; permanent magnet; static eccentricity; synchronous generator

1. Introduction

Eccentricity and demagnetization are two critical mechanical faults that can both occur in electrical machines, creating vital problems in the industry. Eccentricity appears when the stator is not placed correctly in relation to the rotor, a phenomenon that can occur during assembly or during machine operation. In other words, eccentricity is the result of manufacturing imperfections like unbalanced mass, poor alignment and excessive tolerances. 60% of the faults that appear in electrical machines are mechanical and 80% of them can create eccentricity [1]. This fault is responsible for unbalanced magnetic forces, vibration, and acoustic noise, creating problems in the machine operation and reducing its lifetime. If the level of eccentricity severity is quite high, stator and rotor can both be scraped, leading to the damage of the generator. Especially, the Axial Flux Permanent Magnet (AFPM) synchronous machines are prone to eccentricity fault because their overall axial length is short and as consequence, the ratio of machine diameter to length is high [2]. In addition, this type of machine contains permanent magnets that can get demagnetized or crack easily. The high temperatures, the structural defects, and the degradation of the coercive force are responsible for this fault. The demagnetization can be partial or total irreversible. The early diagnosis of both faults is a vital need for the interrupted operation of the systems in the industry.

In the international literature, several methods are proposed for demagnetization [3–6] and eccentricity detection [5–7]. The most commonly used methods are the Time Domain, the Frequency

Analysis, and the Time Scale Analysis Methods, like Discrete or Continuous Wavelet Transform. The Motor Current Signature Analysis (MCSA) and the Motor Voltage Current Analysis (MVCA) are the most frequently used online methods for fault detection, since there is no need for any additional connections or hardware.

The majority of existing studies investigates these faults in Radial Flux Permanent Magnet (RFPM) synchronous machines. During recent years, the demagnetization and the eccentricity fault have also been studied in the AFPM synchronous machine. More specifically [2,8–21] study the eccentricity fault, while [21–30] investigate the demagnetization fault in AFPM synchronous machines. In [31] a combined eccentricity and demagnetization fault in a double-sided AFPM synchronous machine using a time analytical model is presented.

This study investigates the partial demagnetization fault, the static eccentricity (angular and axis) faults and the combined partial demagnetization and static eccentricity (angular and axis) faults. The Electromotive Force (EMF) spectrum will be used for fault diagnosis purposes and the fault signatures harmonics will be extracted. The machine simulation is performed while using the three-dimensional (3D)-Finite Element Analysis (FEA) that gives more accurate results for this machine type. In all demagnetized cases, one magnet of the generator is partially demagnetized in different percentages, while the generator speed in constant, 375 rpm. Section 2 portrays the basic characteristics of the AFPM synchronous generator, in which the faults are studied. Section 3 provides a validation of the Finite Element Method (FEM) model of the machine, while Section 4 explains the two different types of eccentricity. Section 5 presents the fault signature analysis and Section 6 investigates the partial demagnetization fault in the AFPM synchronous generator without the coexistence of the static eccentricity. Two percentages of partial demagnetization (50% and 80%) are examined. Section 7 studies the static angular and the static axis eccentricity faults. An additional spectrum, the spectrum of the phase EMF sum, has been used for fault diagnosis cases in this specific section. Subsequently, Section 8 studies the combined fault of partial demagnetization in combination with static angular and static axis eccentricity. The fault related harmonics in the EMF spectra are exported and comparisons are made when the level of partial demagnetization changes and the severity of eccentricities remains constant and when the level of partial demagnetization does not change, but the severity of eccentricities increases. Finally, Section 9 is the conclusion section which summarizes the basic assumptions. The novelty of the paper is that these combined faults have not been previously studied in the international literature as well as the phase EMF sum waveform has not been previously used for fault detection in this type of generator under these specific faults.

2. The AFPM Synchronous Generator

The machine, in which the faults are investigated, is a three phase, star connected with neutral, double-sided rotor AFPM synchronous generator [32]. Figure 1 depicts the axial representation of the generator. The generator has 375 rpm nominal speed, 50 Hz nominal frequency, 80 V nominal voltage, 250 W nominal power, 16 poles in each rotor, 12 coils, and 210 turns per coil. The rotor, the magnet, the airgap, and the stator have 12 mm, 10 mm, 3 mm, and 18 mm axial thicknesses, respectively, while the stator external radius is 158mm and internal 60 mm.

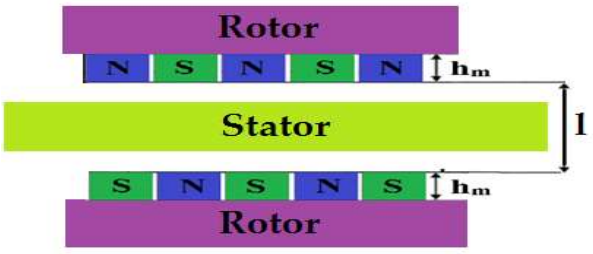

Figure 1. The axial representation of the generator.

Beside the two rotors, there is a coreless stator with concentrated, non-overlapping, and trapezoidal, windings embedded in resin. Figure 2 depicts its layout, where b_{co} is 34.3 mm, b_{ci} is 9 mm, b_{sc} is 16.52 mm, l_c is 63.2 mm, R_i is 58.35 mm, R_o is 121.55 mm, and r is 89.95 mm. Each rotor has 16 permanent magnets of trapezoidal shape made by NdFeB and their layout is presented in Figure 3, where b_{mo} is 47 mm, b_{mi} is 6 mm, R_i is 77.57 mm, R_o is 138.2 mm, and R is 107.885 mm.

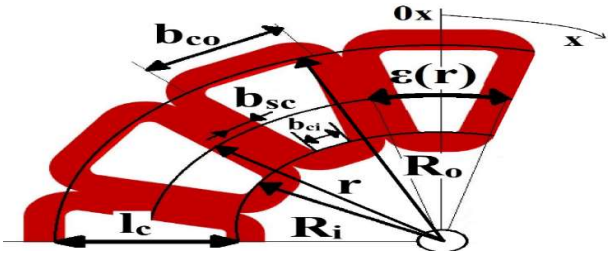

Figure 2. The basic dimension parameters of the generator winding.

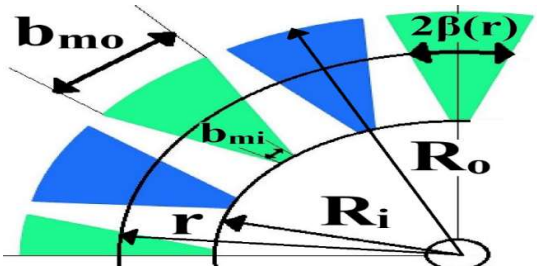

Figure 3. The basic dimension parameters of the permanent magnets of the generator.

In the axial flux permanent magnet synchronous generator, the axial component of the magnetic flux density is divided to the axial component of the magnetic flux density due to the winding Magnetomotive Force (MMF) and the axial component of the magnetic flux density due to the permanent magnets that can be given by (1):

$$B_z = B_{z\_MMF} + B_{z\_PM} \tag{1}$$

where B_z is the axial component of the magnetic flux density in the AFPM, B_{z_MMF} is the axial component of the magnetic flux density due to the winding MMF, and B_{z_PM} is the axial component of the magnetic flux density due to the permanent magnets.

In an AFPM machine with three phases, the axial component of the magnetic flux density due to the MMF can be given by (2):

$$B_{z\_MMF} = \sum_{a=1}^{3} \frac{\mu_0}{1 + 2h_m} F_a \tag{2}$$

where

$$F_a = \sum_{v \in P} i_a \frac{1}{\pi} \frac{w_s}{|v|} \sin\left(|v| \frac{\varepsilon_r}{2}\right) \frac{\sin\left(|v| \frac{a_{sc}(r)}{2}\right)}{|v| \frac{a_{sc}(r)}{2}} e^{jv(x - x_a)} \tag{3}$$

and

$$x_a = (a - 1) \frac{2\pi}{3p_s} \tag{4}$$

where F_α is the MMF of the phase α winding, w_s the number of phase winding turns, p_s the number of phase coils, x the location according to the stator, $\varepsilon(r) = \frac{b_c}{r}$, $b_c \approx \frac{b_{c0} + b_{ci}}{2}$, $a_{sc}(r) = \frac{b_{sc}}{r}$, and P = { … $-3p_s$, $-2p_s$, $-p_s$, p_s, $2p_s$, $3p_s$ … } [33].

The axial component of the magnetic flux density due to the permanent magnets can be given by (5):

$$B_{z\_PM} = \sum_{\varsigma \in Q} \frac{4}{\pi} \frac{B_r}{\varsigma} \frac{h_m}{2h_m + 1} p \sin(\varsigma \beta(r)) e^{j\varsigma(x-\varphi)} \quad (5)$$

where

$$\beta(r) = \frac{b_m}{2r} \quad (6)$$

where $b_m \approx \frac{b_{mo}+b_{mi}}{2}$, φ the angle of a rotor position and Q = { … −5p, −3p, −p, p, 3p, 5p … } [33].

The harmonics that will be created in the magnetic flux density spectrum are responsible for the harmonics that will appear in the EMF spectrum.

3. Model Validation

For the validation of the model in the healthy condition, we present the waveforms of the stator current, derived from the simulation and experiment, respectively, when the machine has nominal speed 375 rpm and supplies the nominal resistive load 70 Ohm, as Figure 4 shows. It can be observed that the two waveforms are qualitatively and quantitatively similar and they validate the accuracy of our FEM model. In addition, Figure 5 depicts the waveforms of the stator current when one magnet is totally demagnetized derived from simulation and experimental procedure when the generator has nominal speed and supplies a load 70 Ohm. It can be seen that the FEM waveform also agrees with the experimental waveform. More specifically, we have used the 3D-Opera mesher while our model contains 5128737 elements. The transient electromagnetic analysis with motion has been used. On a PC (Intel i7-4770 with 8 GB RAM) the finite element analysis requires 12 h in order to reach the steady state condition.

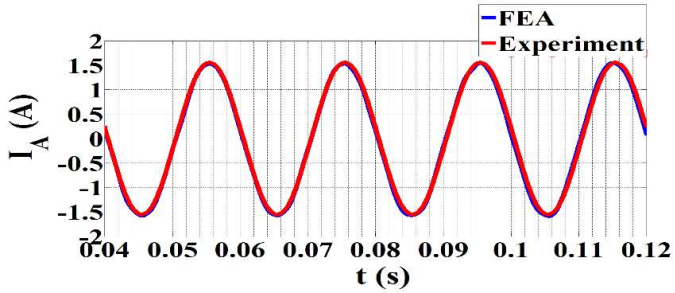

Figure 4. The stator current waveform in the healthy condition when the generator has nominal speed 375 rpm and supplies the nominal load of 70 Ohm (blue line-simulation results, red line-experimental results).

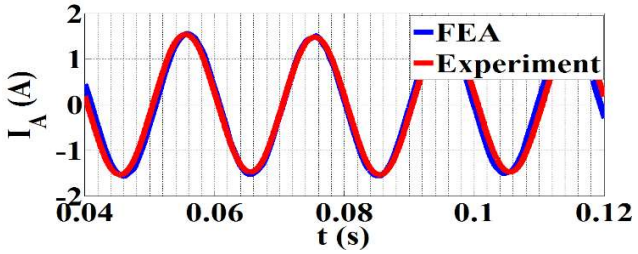

Figure 5. The stator current waveform when one magnet is totally demagnetized, the generator has nominal speed 375 rpm and supplies the nominal load of 70 Ohm (blue line-simulation results, red line-experimental results).

4. Types of Eccentricity

Two types of static eccentricity appear in the literature [15,16]: the static angular and the static axis eccentricity. The first type occurs when the rotor axis coincides with the rotation axis but does not coincide with the stator axis. In this case, the air gap is not uniform, but, during the rotation, the maximum and minimum air gap positions are constant. In other words, the air gap does not change in time. The second type occurs when the stator and rotor are offset from each other in the axis direction. Figure 6 depicts the axial representation of the machine when the two different types of static eccentricity exist in the generator.

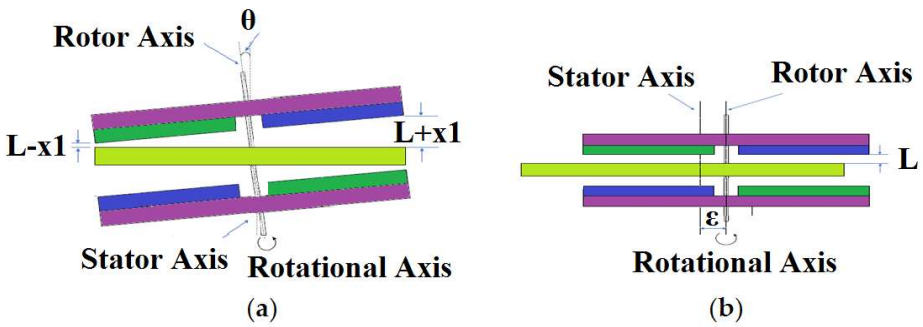

Figure 6. The axial representation of the machine when the generator is: (**a**) static angular eccentric and (**b**) static axis eccentric. Axial representation of the generator.

5. Fault Signature Analysis

From the literature [7,34–36], it is known that the stator current spectrum of a RFPM synchronous machine with demagnetization or eccentricity fault contains new harmonics that are given by Equation (7):

$$f_{demag} = f_s\left(1 \pm \frac{k}{p}\right) \quad (7)$$

where f_{demag} are the frequencies of the fault related harmonics, fs is the fundamental frequency, p the number of machine poles pairs, and k an integer number. Previous studies [29,30] prove that this Equation can predict also the fault related harmonics in the EMF and stator current spectra of an AFPM synchronous machine with totally demagnetized magnets. In this article, it is examined whether this Equation is applicable in the case of the combined fault, in order to interpret the fault related harmonics.

6. Partial Demagnetization

First, the partial demagnetization fault without the coexistence of the eccentricity fault is studied. In all of the investigated cases, one magnet is partially demagnetized in two different percentages (50% and 80% partial demagnetization). Figure 7 depicts the machine 3D-FEA model when one magnet is partially demagnetized, and Figure 8 shows the waveforms of the axial component of the magnetic flux density when the fault exists. The increment of the severity of the demagnetization leads to the decrement of the amplitude of the waveform in the location of the faulty magnet.

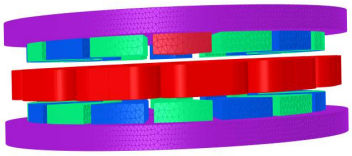

Figure 7. The three-dimensional (3D)-FEA model of the machine when one magnet is partially demagnetized.

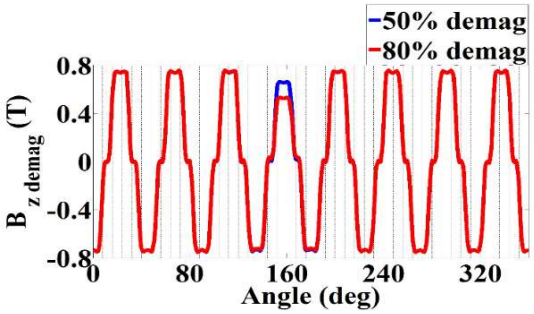

Figure 8. The waveform of the axial component of the magnetic flux density when one magnet is partially demagnetized (blue line—50% partial demagnetization, red line—80% partial demagnetization).

The above waveform can be given by Equation (8) [37]:

$$B_{z\_one\_dem} = B_{z\_tot} - y(t) \tag{8}$$

where B_{z_tot} is the axial component of the total magnetic flux density in the healthy case and y(t) is the product between the B_{z_tot} and the square wave x(t) divided by V_{dem}, which is the B_{z_tot} amplitude immersion due to TDF, as it can be seen by (9):

$$y(t) = \frac{B_{z\_tot}}{V_{dem}} x(t) \tag{9}$$

while x(t) can be expressed in Fourier series using (10):

$$x(t) = \frac{1}{2p} + \sum_{k=1}^{\infty} \frac{2}{k\pi} \sin\left(\frac{\pi k}{2p}\right) \cos\left(\frac{2k\pi f_s t}{p}\right) \tag{10}$$

Substituting (9) and (10) in (8) implies (11):

$$B_{z\_one\_dem} = B_{z\_tot} - \frac{B_{z\_tot}}{2pV_{dem}} - \sum_{k=1}^{\infty} \frac{2B_{z\_tot}}{k\pi V_{dem}} \sin\left(\frac{k\pi}{2p}\right) \cos\left(\frac{2k\pi f_s t}{p}\right) \tag{11}$$

The harmonics that appear in Equation (11) are responsible for the harmonics that will be created in the EMF spectrum in the faulty condition. Equation (11) is suitable to interpret every percentage of partial demagnetization, because, as can been seen below, when the fault severity changes the kind of the fault related harmonics does not change but their amplitude changes. In Equation (11), it will be modification in V_{dem} when the severity of the fault changes.

Figures 9 and 10 depict the EMF waveforms and the corresponding spectra when one magnet is 50% and 80% partially demagnetized. The increment of the fault severity reduces the amplitude of the EMF waveform. In addition, the fault creates new harmonics in the corresponding spectra, which Table 1 summarizes. The new harmonics are of frequencies 25 Hz, 75 Hz, 100 Hz, 125 Hz, 175 Hz, 200 Hz, and 225 Hz and their amplitudes increase when the severity of demagnetization increases. The fundamental harmonic decreases in amplitude when the level of demagnetization increases. The fault related harmonics are both even and fractional and of the same frequencies, like the case wjere one magnet is totally demagnetized [30].

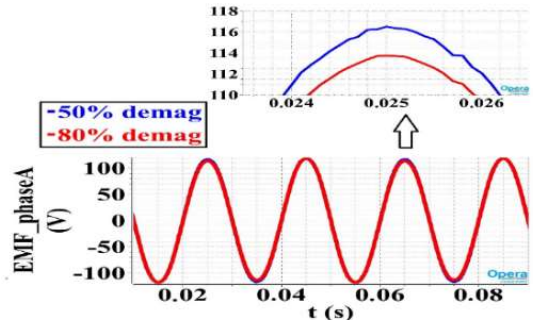

Figure 9. The EMF waveform when one magnet is partially demagnetized (blue line—50% partial demagnetization, red line—80% partial demagnetization).

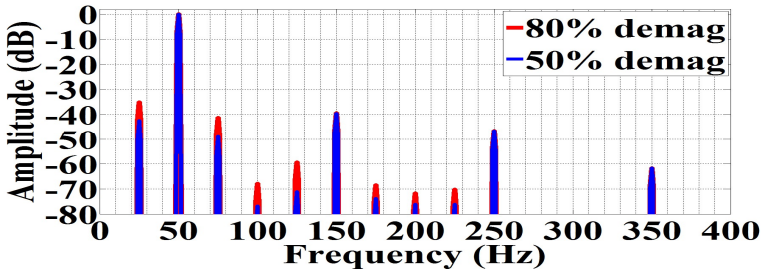

Figure 10. The EMF spectrum when one magnet is partially demagnetized (blue line—50% partial demagnetization, red line-80% partial demagnetization).

Table 1. Fundamental Harmonic and Fault Related Harmonics in the Spectrum of the EMF When One Magnet is Partially Demagnetized.

Harmonic Order	F (Hz)	Generator with One 50% Partially Demagnetized Magnet		Generator with One 80% Partially Demagnetized Magnet	
		(dB)	(V)	(dB)	(V)
0.5	25	−42.33	0.2455	−35.10	0.5581
1	50	0	32.12	0	31.74
1.5	75	−48.88	0.1156	−41.29	0.2733
2	100	−76.84	0.004686	−67.97	0.01299
2.5	125	−71.04	0.009101	−59.38	0.03411
3.5	175	−73.79	0.006643	−68.48	0.01198
4	200	−76.03	0.00501	−71.77	0.008362
4.5	225	−76.1	0.005209	−70.28	0.00991

7. Static Eccentricity Fault

7.1. Static Angular Eccentricity Fault

In this section, the static angular eccentricity fault will be studied. As it is already proven in [18], the static angular eccentricity fault does not create new harmonics in the EMF and the stator current spectra. This can be justified by the fact that during this fault the airgap in a double-sided machine increases from the one side and decreases from the other size resulting in a constant total airgap. For that reason, the EMF waveform, the stator current waveform, and the corresponding spectra remain approximately unaffected by the fault. However, the spectrum of the phase EMF sum presents variation when static angular eccentricity exists in the generator. Figure 11 depicts the phase EMF sum spectra for two different severities of static angular eccentricity (30% and 40%). Equation (12) describes the phase EMF sum waveform. This signal has a fundamental frequency of 150 Hz ($3f_s$), three times the fundamental frequency of the EMF waveform of each generator phase (f_s). In both cases, the harmonic component of frequency 50Hz is the fault related harmonic that, in the faulty case, its amplitude

increases more than the other amplitudes when compared to the corresponding healthy spectrum for spectra normalized to the $3f_s$ frequency (150 Hz). When the level of eccentricity increases, the amplitude of this harmonic component also increases, as can be seen by Table 2. In other words, we can tell that the component of frequency f_s Hz is the most dominant fault related harmonic component in the EMF sum spectrum and it indicates the existence of static angular eccentricity fault. Finally, from Table 2, it can be seen that the absolute value of the $3f_s$ harmonic component (150 Hz) also increases when the eccentricity severity increases.

$$PhaseEMF_{sum} = EMF_{phaseA} + EMF_{phaseB} + EMF_{phaseC} \quad (12)$$

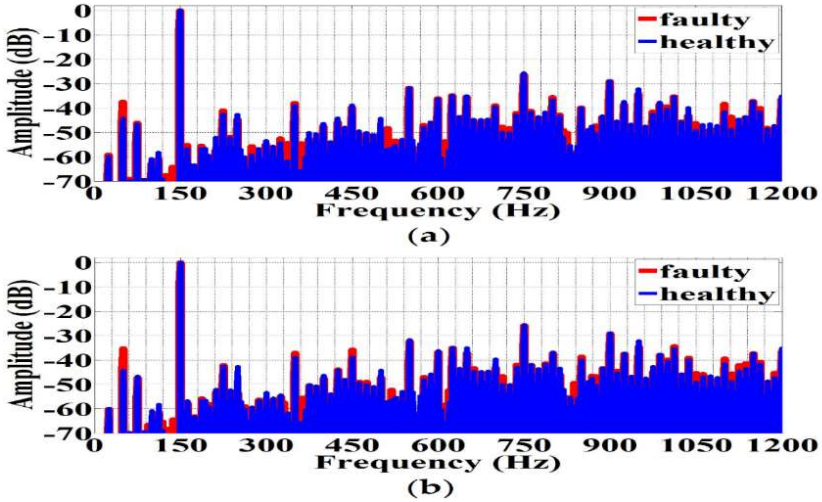

Figure 11. The phase EMF sum spectra of the double-sided rotor generator when a static angular eccentricity exists in the machine: (**a**) 30% fault severity, (**b**) 40% fault severity. (blue line-healthy case, red line-faulty case).

Table 2. The Harmonics of Frequencies 50 Hz and 150 Hz in the Spectrum of the phase EMF sum When Static Angular Eccentricity exists in the Generator.

Harmonic	f (Hz)	Healthy Generator		Generator with 30% Static Angular Eccentricity		Generator with 40% Static Angular Eccentricity	
		(dB)	(V)	(dB)	(V)	(dB)	(V)
f_s	50	−44.33	0.00634	−37.51	0.01392	−35.29	0.01816
$3f_s$	150	0	1.043	0	1.045	0	1.056

7.2. Static Axis Eccentricity Fault

In this section, the static axis eccentricity fault will be studied. Like with the previous case, the static axis eccentricity fault does not create new harmonics in the phase EMF and the stator current spectra. In [18], it is referred that, when the severity of eccentricity increases, the amplitude of the third harmonic of the phase EMF spectrum slightly increases, while the amplitudes of the fifth and seventh harmonics slightly decrease. However, in the phase EMF sum, new harmonic components appear as Figure 12 depicts. As it can be observed, the harmonic component of frequency f_s Hz is a fault related harmonic, like to the case of static angular eccentricity. Consequently, the increment of the amplitude of the harmonic component of 50 Hz indicates static eccentricity fault but we cannot separate the two faults. Finally, Table 3 summarizes the amplitude in dB and in absolute value of the harmonic components of frequencies 50 Hz and 150 Hz.

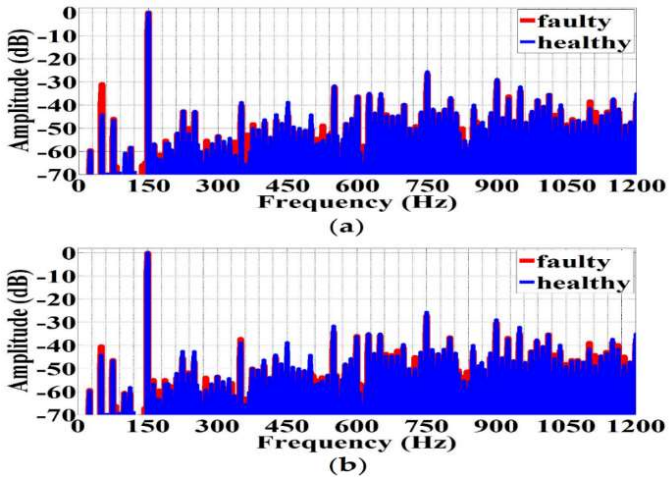

Figure 12. The phase EMF sum spectra of the double-sided rotor generator when a static axis eccentricity exists in the machine: (**a**) 2mm fault severity, (**b**) 3mm fault severity (blue line—healthy case, red line—faulty case).

Table 3. The Harmonics of Frequencies 50 Hz and 150 Hz in the Spectrum of the phase EMF sum When Static Axis Eccentricity exists in the Generator.

Harmonic f (Hz)		Healthy Generator		Generator with 2mm Static Axis Eccentricity (dB)		Generator with 3mm Static Axis Eccentricity (dB)	
		(dB)	(V)	(dB)	(V)	(dB)	(V)
f_s	50	−44.33	0.00634	−31.01	0.03033	−40.47	0.01051
$3f_s$	150	0	1.043	0	1.077	0	1.109

8. The Combined Fault

8.1. The Combined Partial Demagnetization and Static Angular Eccentricity Fault

In this paragraph, the combined partial demagnetization and static angular eccentricity fault is studied. In all cases, one magnet is partially demagnetized. Figure 13 depicts the EMF spectra when the severity of static angular eccentricity remains constant and the level of demagnetization changes, while Figure 14 shows the EMF spectra when the level of demagnetization remains constant and the severity of static angular eccentricity changes. Although the static angular eccentricity does not create new harmonics in this spectrum [18], when it is combined with demagnetization, new harmonic components appear. The new harmonics due to the combined fault agree with Equation (7) for k =−5, −4, −3, −1, 1, 3, 4, 5, 8, 12, 20, 24, 28. The machine odd harmonics (third, fifth, and seventh) appear variation when the combined fault exists. More specifically, the amplitude of the third harmonic decreases when there is combined fault in the machine, while the amplitudes of the fifth and seventh harmonics increase, like the case that only static angular eccentricity exists in the generator [18]. In other words, the variation of the amplitude of these harmonic components is due to static angular eccentricity fault. Tables 4 and 5 summarize the amplitudes of the fault related harmonics derived from Figures 13 and 14 respectively. As it can be seen by Table 4, when the demagnetization level increases and the static angular eccentricity level remains constant, the amplitude of all combined fault related harmonics also increases. However, the absolute value of the fundamental frequency, 50 Hz, slightly decreases. Observing Table 5, we can see that when the severity of the partial demagnetization remains invariable and the level of static angular eccentricity increases the amplitude of all combined fault related harmonics increases too with exception the demagnetization fault related harmonics. In other words, the increment of the eccentricity also creates an increment of the amplitude of the harmonics with frequencies 18.75 Hz, 31.25 Hz, 43.75 Hz, 56.25 Hz, 68.75 Hz, 81.25 Hz. The amplitude of the demagnetization harmonic components (0.5th, 1.5th, 2nd, 2.5th, 3.5th, 4th, and 4.5th) remains approximately constant, as expected when taking

into consideration that the level of demagnetization does not change. In addition, the absolute value of the fundamental frequency presents slightly increment, as Table 5 depicts.

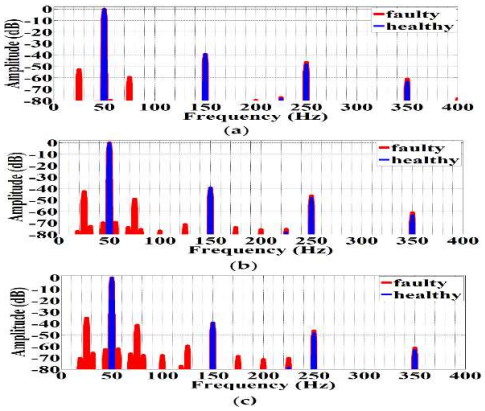

Figure 13. The EMF spectra when a combined fault of partial demagnetization and static angular eccentricity exists in the generator and the level of demagnetization changes: (**a**) 20% demagnetization and 30% static angular eccentricity, (**b**) 50% demagnetization and 30% static angular eccentricity, and (**c**) 80% demagnetization and 30% static angular eccentricity.

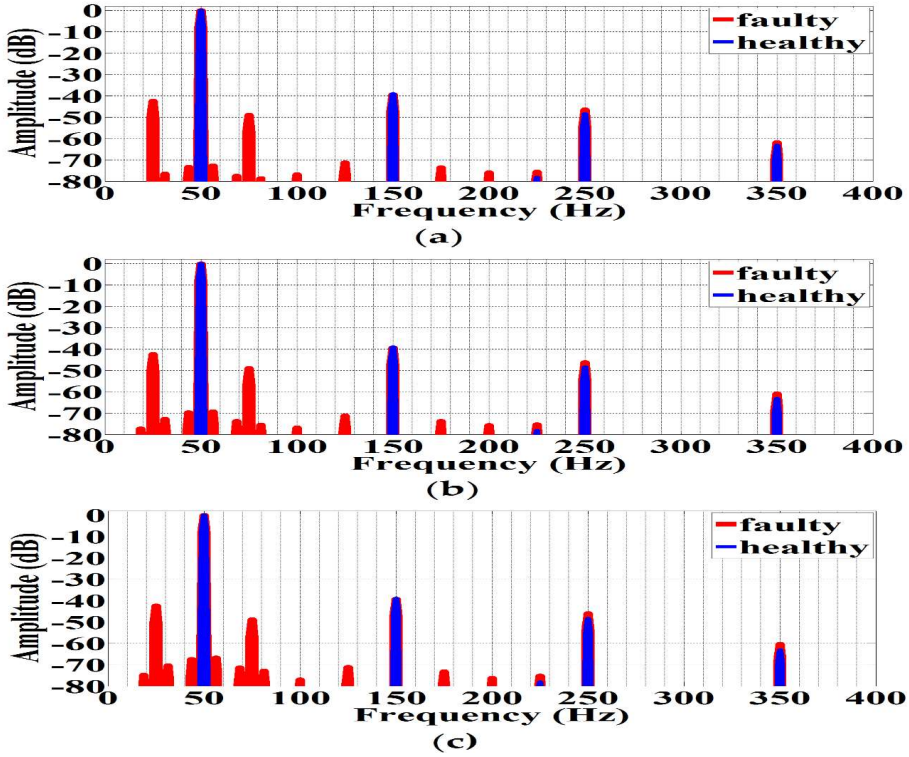

Figure 14. The EMF spectra when a combined fault of partial demagnetization and static angular eccentricity exists in the generator and the level of eccentricity changes: (**a**) 50% demagnetization and 20% static angular eccentricity, (**b**) 50% demagnetization and 30% static angular eccentricity, and (**c**) 50% demagnetization and 40% static angular eccentricity.

Table 4. Fundamental and Fault Related Harmonics in the Spectrum of the EMF for the Combined Partial Demagnetization and Static Angular Eccentricity Fault When Changes the Level of Demagnetization.

Harmonic Order	f (Hz)	Healthy Generator		Generator with One 20% Partially Demagnetized Magnet and 30% Static Angular Eccentricity		Generator with One 50% Partially Demagnetized Magnet and 30% Static Angular Eccentricity		Generator with One 80% Partially Demagnetized Magnet and 30% Static Angular Eccentricity	
		(dB)	(V)	(dB)	(V)	(dB)	(V)	(dB)	(V)
0.375	18.75	-	5.366×10^{-5}	-	0.001382	−77.24	0.004418	−70.1	0.009934
0.5	25	-	0.00219	−52.52	0.07655	−42.35	0.2452	−35.1	0.5586
0.625	31.25	-	2.246×10^{-5}	-	0.002323	−72.76	0.007402	−65.6	0.01669
0.875	43.75	-	8.122×10^{-5}	−79.67	0.003362	−69.71	0.01052	−62.51	0.02379
1	50	0	32.07	0	32.36	0	32.16	0	31.78
1.125	56.25	-	5.785×10^{-5}	−79.35	0.003489	−69.18	0.01117	−61.86	0.02566
1.375	68.75	-	0.0002289	-	0.002056	−73.73	0.006621	−68.75	0.01541
1.5	75	-	0.001492	−59.27	0.03521	−48.87	0.1158	−41.29	0.2739
1.625	81.25	-	0.0001917	-	0.00158	−75.43	0.005441	−67.7	0.0131
2	100	-	0.001133	-	0.001901	−76.74	0.004682	−67.75	0.01302
2.5	125	-	0.0009809	-	0.001735	−71.1	0.008965	−59.4	0.03406
3.5	175	-	0.0006477	-	0.002879	−73.7	0.006641	−68.56	0.01186
4	200	-	0.001959	−79.36	0.003483	−75.64	0.005314	−71.25	0.008699
4.5	225	−78.11	0.003984	−76.9	0.004623	−75.35	0.00549	−70.03	0.01001

Table 5. Fundamental and Fault Related Harmonics in the Spectrum of the EMF for the Combined Partial Demagnetization and Static Angular Eccentricity Fault When Changes the Level of Eccentricity.

Harmonic Order	F (Hz)	Healthy Generator		Generator with One 50% Partially Demagnetized Magnet and 20% Static Angular Eccentricity		Generator with One 50% Partially Demagnetized Magnet and 30% Static Angular Eccentricity		Generator with One 50% Partially Demagnetized Magnet and 40% Static Angular Eccentricity	
		(dB)	(V)	(dB)	(V)	(dB)	(V)	(dB)	(V)
0.375	18.75	-	5.366×10^{-5}	-	0.002912	−77.24	0.004418	−74.76	0.005873
0.5	25	-	0.00219	−42.33	0.2456	−42.35	0.2452	−42.35	0.2458
0.625	31.25	-	2.246×10^{-5}	−76.4	0.004863	−72.76	0.007402	−70.34	0.009796
0.875	43.75	-	8.122×10^{-5}	−73.24	0.006998	−69.71	0.01052	−67.39	0.01375
1	50	0	32.07	0	32.13	0	32.16	0	32.2
1.125	56.25	-	5.785×10^{-5}	−72.59	0.005742	−69.18	0.01117	−66.75	0.01481
1.375	68.75	-	0.0002289	−77.46	0.004302	−73.73	0.006621	−71.39	0.008676
1.5	75	-	0.001492	−48.87	0.1157	−48.87	0.1158	−48.85	0.1163
1.625	81.25	-	0.0001917	−78.57	0.003786	−75.43	0.005441	−72.82	0.007364
2	100	-	0.001133	−76.76	0.004668	−76.74	0.004682	−76.98	0.004557
2.5	125	-	0.0009809	−71.22	0.008831	−71.1	0.008965	−71.18	0.008893
3.5	175	-	0.0006477	−73.55	0.00675	−73.7	0.006641	−73.21	0.007038
4	200	-	0.001959	−75.9	0.00515	−75.64	0.005314	−76.18	0.004998
4.5	225	−78.11	0.003984	−75.53	0.005375	−75.35	0.00549	−75.16	0.005619

8.2. The Combined Partial Demagnetization and Static Axis Eccentricity Fault

This paragraph investigates the combined partial demagnetization with static axis eccentricity fault. Figure 15 presents the EMF spectra for the combined fault when the level of static axis eccentricity remains constant and the severity of demagnetization changes, while Figure 16 depicts the EMF spectra for the combined fault when the level of demagnetization remains constant and the level of static axis eccentricity changes. The corresponding amplitudes of the combined fault related harmonics are depicted in Tables 6 and 7, respectively. The combined fault creates new harmonic components in the EMF spectra, in contrast to the case that only static axis eccentricity exists in the generator and in the EMF spectrum do not appear new harmonic components that are related to the fault, as [18] proves. The combined fault related harmonics are of frequencies 18.75 Hz, 25 Hz, 31.25 Hz, 43.75 Hz, 56.25 Hz, 68.75 Hz, 75 Hz, 81.25 Hz, 100 Hz, 125 Hz, 175 Hz, 200Hz, and 225 Hz. These harmonics agree with Equation (7) for k = −5, −4, −3, −1, 1, 3, 4, 5, 8, 12, 20, 24, and 28, like in the previous section, Section 8.1. In other words, in two combined faults appear the same fault related harmonics. The machine odd harmonics (third, fifth, and seventh) remain approximately constant when the combined fault exists when compared to the healthy case, like to the case that only static axis eccentricity exists in the generator [18]. Observing Table 6, it can be seen that, when the severity of demagnetization increases while the level of static axis eccentricity remains constant, the amplitude of the combined fault related harmonics also increases, like the case where a combined partial demagnetization and static angular eccentricity fault exists in the generator. Although the absolute value of the fundamental frequency presents a small decrement, as Table 6 depicts. Table 7 shows that, when the level of demagnetization remains invariable and the severity of static axis eccentricity increases, the amplitude of all combined fault related harmonics slightly increases apart from the harmonic components with frequencies 25 Hz, 75 Hz, 100 Hz, 125 Hz, 175 Hz, 200 Hz, and 225 Hz. These components are related with demagnetization and for that reason do not change amplitude when the demagnetization level is constant, like Section 8.1. Finally the absolute value of the fundamental frequency slightly decreases when changes the level of the eccentricity and the demagnetization level remains constant. To conclude, it can be observed that when only partial demagnetization exists on the generator, fault related harmonics of frequencies of 25 Hz, 75 Hz, 100 Hz, 125 Hz, 175 Hz, 200 Hz, and 225 Hz appear in the EMF spectrum, when only static eccentricity, either angular or axis, exists do not appear new harmonics in the EMF spectrum, while, in the cases of combined faults, fault related harmonics of frequencies 18.75 Hz, 25 Hz, 31.25 Hz, 43.75 Hz, 56.25 Hz, 68.75 Hz, 75 Hz, 81.25 Hz, 100 Hz, 125 Hz, 175 Hz, 200Hz, and 225 Hz appear. In other words, in the last cases, the demagnetization fault related harmonics and some sideband harmonics appear. The phase EMF sum signal can also be used in the case of combined faults, but the reason that we did not investigate it is because the EMF signal is able to provide the fault related harmonics that are related to combined faults, in contrast to Section 7. The fault identification using the EMF signal and not the phase EMF sum signal makes the detection process simpler and more cost effective, as we should measure one signal every time and not three different signals. However, the study of the phase EMF sum signal in combined faults can be an object of investigation in a future article.

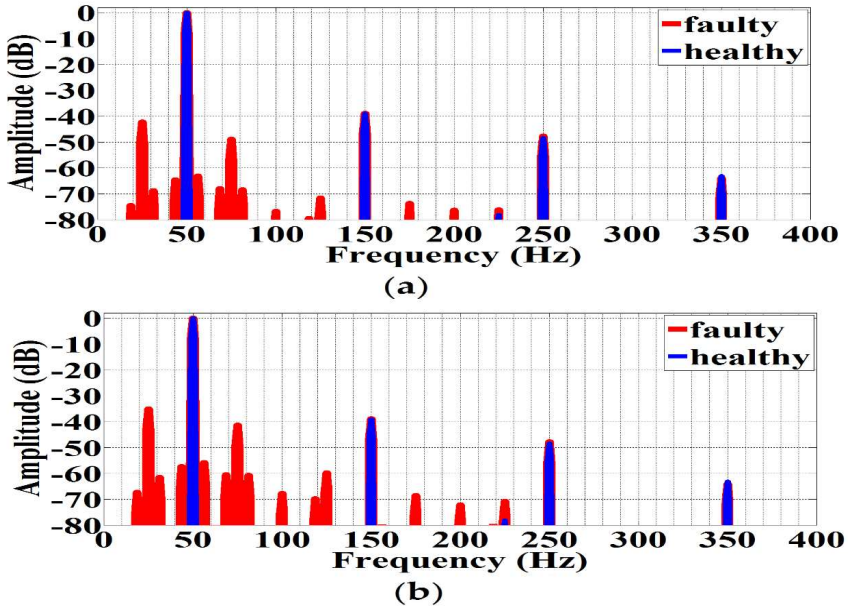

Figure 15. The EMF spectra when a combined fault: (**a**) 50% demagnetization and 2 mm static axis eccentricity, (**b**) 80% demagnetization and 2 mm static axis eccentricity exist in the generator.

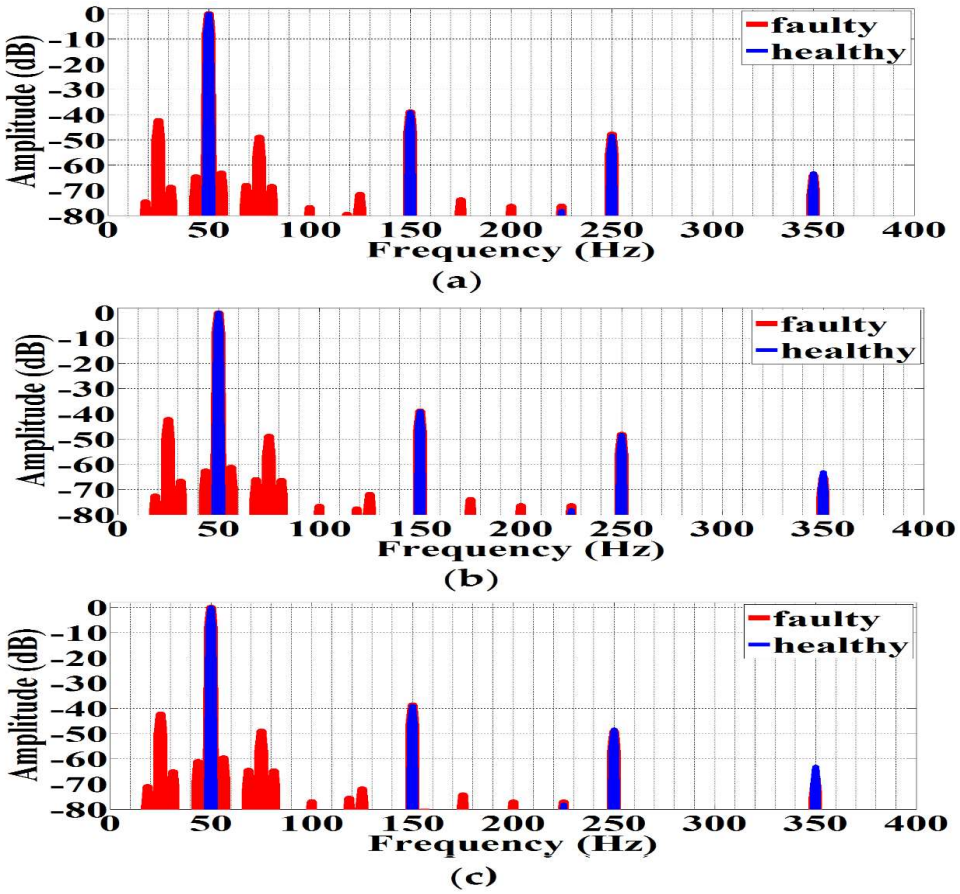

Figure 16. The EMF spectra when a combined fault: (**a**) 50% demagnetization and 2 mm static axis eccentricity, (**b**) 50% demagnetization and 2.5 mm static axis eccentricity, and (**c**) 50% demagnetization and 3 mm static axis eccentricity exist in the generator.

Table 6. Fundamental and Fault Related Harmonics in the Spectrum of the EMF for the Combined Partial. Demagnetization and Static Axis Eccentricity Fault When Changes the Level of Demagnetization.

Harmonic Order	f (Hz)	Healthy Generator		Generator with One 50% Partially Demagnetized Magnet and 2mm Static Axis Eccentricity		Generator with One 80% Partially Demagnetized Magnet and 2mm Static Axis Eccentricity	
		(dB)	(V)	(dB)	(V)	(dB)	(V)
0.375	18.75	-	5.366×10^{-5}	−74.56	0.005965	−67.27	0.01365
0.5	25	-	0.00219	−42.3	0.2448	−35.06	0.5566
0.625	31.25	-	2.246×10^{-5}	−68.75	0.01165	−61.59	0.02624
0.875	43.75	-	8.122×10^{-5}	−64.64	0.01869	−57.39	0.04255
1	50	0	32.07	0	31.89	0	31.52
1.125	56.25	-	5.785×10^{-5}	−63.1	0.02231	−55.78	0.05123
1.375	68.75	-	0.0002289	−67.99	0.01271	−60.57	0.02951
1.5	75	-	0.001492	−48.95	0.1139	−41.36	0.2694
1.625	81.25	-	0.0001917	−68.4	0.01212	−60.73	0.02897
2	100	-	0.001133	−76.79	0.004618	−67.78	0.01287
2.5	125	-	0.0009809	−71.59	0.008395	−59.72	0.03254
3.5	175	-	0.0006477	−73.73	0.006561	−68.59	0.01172
4	200	-	0.001959	−76.38	0.004839	−72.15	0.007781
4.5	225	−78.11	0.003984	−76.22	0.004926	−70.75	0.00914

Table 7. Fundamental and Fault Related Harmonics in the Spectrum of the EMF for the Combined Partial Demagnetization and Static Axis Eccentricity Fault When Changes the Level of Eccentricity.

Harmonic Order	f (Hz)	Healthy Generator		Generator with One 50% Partially Demagnetized Magnet and 2mm Static Axis Eccentricity		Generator with One 50% Partially Demagnetized Magnet and 2.5mm Static Axis Eccentricity		Generator with One 50% Partially Demagnetized Magnet and 3mm Static Axis Eccentricity	
		(dB)	(V)	(dB)	(V)	(dB)	(V)	(dB)	(V)
0.375	18.75	-	5.366×10^{-5}	−74.56	0.005965	−72.63	0.007425	−70.99	0.008928
0.5	25	-	0.00219	−42.3	0.2448	−42.28	0.2445	−42.26	0.2439
0.625	31.25	-	2.246×10^{-5}	−68.75	0.01165	−66.8	0.01454	−65.21	0.01739
0.875	43.75	-	8.122×10^{-5}	−64.64	0.01869	−62.73	0.02323	−61.21	0.02782
1	50	0	32.07	0	31.89	0	31.79	0	31.66
1.125	56.25	-	5.785×10^{-5}	−63.1	0.02231	−61.19	0.02773	−59.6	0.03313
1.375	68.75	-	0.0002289	−67.99	0.01271	−66.02	0.0159	−64.55	0.01875
1.5	75	-	0.001492	−48.95	0.1139	−48.98	0.1131	−49.02	0.1121
1.625	81.25	-	0.0001917	−68.4	0.01212	−66.4	0.01522	−64.79	0.01823
2	100	-	0.001133	−76.79	0.004618	−76.66	0.004671	−77.04	0.00445
2.5	125	-	0.0009809	−71.59	0.008395	−71.92	0.008061	−71.93	0.008013
3.5	175	-	0.0006477	−73.73	0.006561	−74.01	0.006336	−74.28	0.006118
4	200	-	0.001959	−76.38	0.004839	−76.5	0.004758	−77.16	0.004392
4.5	225	−78.11	0.003984	−76.22	0.004926	−76.48	0.004767	−77.1	0.00442

9. Conclusions

This paper investigates the partial demagnetization fault, the static angular and the static axis eccentricity fault, and the combination of partial demagnetization and static angular or static axis eccentricity fault in an AFPM synchronous double-sided rotor generator. The machine has been simulated while using 3D-FEA, while the EMF spectra are studied for fault diagnosis purposes in order to extract the fault related harmonics. In all cases one magnet is partially demagnetized. Firstly, the partial demagnetization fault without the coexistence of eccentricity is studied for two

different percentages of partial demagnetization. This fault creates both even and fractional harmonics (with frequencies of 25 Hz, 75 Hz, 100 Hz, 125 Hz, 175 Hz, 200 Hz, and 225 Hz) in the EMF spectra and the harmonic amplitude increases when the severity of partial demagnetization also increases. In addition, the static angular and the static axis eccentricity faults are investigated. Both of the faults do not create new harmonics in the corresponding EMF spectra. However, these faults create new harmonic components in the phase EMF sum spectrum. The phase EMF sum waveform is a signal that has a fundamental frequency of 150 Hz ($3f_s$), three times the fundamental frequency, f_s, of the EMF waveform. When static eccentricity fault exists, either angular or axis, in the corresponding spectra of the phase EMF sum new harmonic components appear and harmonic component of frequency 50 Hz is the fault related harmonic component that, in the faulty case, its amplitude increases more than the amplitudes of other harmonics when compared to the corresponding healthy spectrum. In other words, this harmonic component in the phase EMF sum spectrum can predict eccentricity, but cannot identify whether the static eccentricity is angular or axis. Then the combined fault of partial demagnetization with static angular eccentricity is studied. The analysis proves that this fault creates new harmonics of frequencies 18.75 Hz, 25 Hz, 31.25 Hz, 43.75 Hz, 56.25 Hz, 68.75 Hz, 75 Hz, 81.25 Hz, 100 Hz, 125 Hz, 175 Hz, 200Hz, and 225 Hz in the EMF spectrum when compared to the healthy case. Comparisons are made when the level of demagnetization changes and the level of eccentricity remains constant and when the level of demagnetization remains constant and the level of eccentricity changes. In the first case, the amplitude of all fault related harmonics increases when the severity of demagnetization increases, while, in the second case, when the severity of eccentricity increases, the amplitude of the fault related harmonics increases too apart from the harmonics that also appear when only demagnetization exist in the machine (0.5th, 1.5th, 2nd, 2.5th, 3.5th, 4th, and 4.5th). In addition, the combined partial demagnetization and static axis eccentricity fault is studied. The fault related harmonics are of frequencies 18.75 Hz, 25 Hz, 31.25 Hz, 43.75 Hz, 56.25 Hz, 68.75 Hz, 75 Hz, 81.25 Hz, 100 Hz, 125 Hz, 175 Hz, 200Hz, and 225 Hz. Like previous cases, comparisons are made when the level of demagnetization increases, and the severity of eccentricity remains constant and when the level of demagnetization remains invariable and the level of static axis eccentricity changes. In the first case, all of the combined fault related harmonics increase in amplitude, while, in the second case, there is increment in the amplitude of all harmonic components apart from these that are related to demagnetization fault. A future step of this study is to find a formula that is able to separate the two eccentricity cases, because, as can be seen in both eccentricity faults, fault related harmonics of the same frequencies appear.

Author Contributions: The presented work was carried out through the cooperation of all authors. A.C.B. conducted the research and wrote the paper and J.C.K. supervised the whole study and edited the manuscript. All authors have read and agreed to the published version of the manuscript.

Funding: This research received no external funding.

Conflicts of Interest: The authors declare no conflict of interest.

References

1. Mirimani, S.M.; Vahedi, A.; Marignetti, F.; De Santis, E. Static Eccentricity Fault Detection in Single-Stator–Single-Rotor Axial-Flux Permanent-Magnet Machines. *IEEE Trans. Ind. Appl.* **2012**, *48*, 1838–1845. [CrossRef]
2. Mirimani, S.M.; Vahedi, A.; Marignetti, F.; Di Stefano, R. An Online Method for Static Eccentricity Fault Detection in Axial Flux Machines. *IEEE Trans. Ind. Electron.* **2015**, *62*, 1931–1942. [CrossRef]
3. Faiz, J.; Nejadi-Koti, H. Demagnetization fault indexes in permanent magnet synchronous motors—An Overview. *IEEE Trans. Magnet.* **2016**, 52. [CrossRef]
4. Faiz, J.; Mazaheri Tehrani, E. Demagnetization modeling and fault diagnosing techniques in permanent magnet machines under stationary and non-stationary conditions an overview. *IEEE Trans. Ind. Appl.* **2016**, *51*, 2772–2785. [CrossRef]

5. Capolino, G.-A.; Antonino-Daviu, J.A.; Riera-Guasp, M. Modern Diagnostics Techniques for Electrical Machines, Power Electronics, and Drives. *IEEE Trans. Ind. Electron.* **2015**, *62*, 1738–1745. [CrossRef]
6. Duan, Y.; Toliyat, H. A Review of Condition Monitoring and Fault Diagnosis for Permanent Magnet Machines. In Proceedings of the 2012 IEEE Power and Energy Society General Meeting, San Diego, CA, USA, 22–26 July 2012.
7. Ebrahimi, B.M.; Faiz, J.; Roshtkhari, M.J. Static-, Dynamic-, and Mixed-Eccentricity Fault Diagnoses in Permanent-Magnet Synchronous Motors. *IEEE Trans. Ind. Electron.* **2009**, *56*, 4727–4739. [CrossRef]
8. Tarek, M.T.B.; Das, S.; Sozer, Y. Comparative Analysis of Static Eccentricity Faults of Double Stator Single Rotor Axial Flux Permanent Magnet Motors. In Proceedings of the 2019 Energy Conversion Congress and Exposition (ECCE), Baltimore, MD, USA, 29 September–3 October 2019.
9. Mirimani, S.M.; Vahedi, A.; Marignetti, F. Effect of Inclined Static Eccentricity Fault in Single Stator-Single Rotor Axial Flux Permanent Magnet Machines. *IEEE Trans. Magnet.* **2012**, *48*, 143–149. [CrossRef]
10. Marignetti, F.; Vahedi, A.; Mirimani, S.M. An Analytical Approach to Eccentricity in Axial Flux Permanent Magnet Synchronous Generators for Wind Turbines. *Electr. Power Componets Syst.* **2015**, *43*, 1039–1050. [CrossRef]
11. Ogidi, O.O.; Barendse, P.S.; Khan, M.A. Detection of Static Eccentricities in Axial-Flux Permanent-Magnet Machines with Concentrated Windings Using Vibration Analysis. *IEEE Trans. Ind. Appl.* **2015**, *51*, 4425–4434. [CrossRef]
12. Ogidi, O.O.; Barendse, P.S.; Khan, M.A. Fault diagnosis and condition monitoring of axial-flux permanent magnet wind generators. *Electr. Power Syst. Res.* **2016**, *136*, 1–7. [CrossRef]
13. Huang, Y.; Guo, B.; Hemeida, A.; Sergeant, P. Analytical Modeling of Static Eccentricities in Axial Flux Permanent-Magnet Machines with Concentrated Windings. *Energies* **2016**, *9*, 892. [CrossRef]
14. Ogidi, O.O.; Barendse, P.S.; Khan, M.A. Influence of Rotor Topologies and Cogging Torque Minimization Techniques in the Detection of Static Eccentricities in Axial-Flux Permanent-Magnet Machine. *IEEE Trans. Ind. Appl.* **2017**, *53*, 161–170. [CrossRef]
15. Thiele, M.; Heins, G. Computationally Efficient Method for Identifying Manufacturing Induced Rotor and Stator Misalignment in Permanent Magnet Brushless Machines. *IEEE Trans. Ind. Appl.* **2016**, *48*, 3033–3040. [CrossRef]
16. Guo, B.; Huang, Y.; Peng, F.; Guo, Y.; Zhu, J. Analytical Modeling of Manufacturing Imperfections in Double-Rotor Axial Flux PM Machines: Effects on Back EMF. *IEEE Trans. Magnet.* **2017**, 53. [CrossRef]
17. Barmpatza, A.C.; Kappatou, J.C.; Skarmoutsos, G.A. Investigation of Static Angular and Axis Misalignment in an AFPM Generator. In Proceedings of the 2019 IEEE Workshop on Electrical Machines Design, Control and Diagnosis (WEMDCD), Athens, Greece, 22–23 April 2019.
18. Barmpatza, A.C.; Kappatou, J.C. A Study of Static Angular and Axis Eccentricity in a Double-Sided Rotor AFPM Generator using 3D-FEM. In Proceedings of the 2019 IEEE International Symposium on Diagnostics for Electrical Machines, Power Electronics and Drives (SDEMPED), Toulouse, France, 27–30 August 2019.
19. Di Gerlando, A.; Foglia, G.M.; Iacchetti, M.F.; Perini, R. Effects of Manufacturing Imperfections in Concentrated Coil Axial Flux PM Machines: Evaluation and Tests. *IEEE Trans. Ind. Electron.* **2014**, *61*, 5012–5024. [CrossRef]
20. Guo, B.; Huang, Y.; Peng, F.; Dong, J.; Li, Y. Analytical Modelling of Misalignment in Axial Flux Permanent Magnet Machine. *IEEE Trans. Ind. Electron* **2020**, *67*, 4433–4443. [CrossRef]
21. Ajily, E.; Ardebili, M.; Abbaszadeh, K. Magnet defect and rotor eccentricity modeling in axial-flux permanent-magnet machines via 3-D Field Reconstruction Method. *IEEE Trans. Energy Convers.* **2016**, *31*, 486–495. [CrossRef]
22. Guo, B.; Huang, Y.; Peng, F.; Dong, J. General Analytical Modeling for Magnet Demagnetization in Surface Mounted Permanent Magnet Machines. *IEEE Trans. Ind. Electron.* **2019**, *66*, 5830–5838. [CrossRef]
23. Verkroost, L.; De Bisschop, J.; Vansompel, H.; De Belie, F.; Sergeant, P. Active Demagnetization Fault Compensation for Axial Flux Permanent Magnet Synchronous Machines Using an Analytical Inverse Model. *IEEE Trans. Energy Convers.* **2020**, *35*, 591–599. [CrossRef]
24. De Bisschop, J.; Abou-Elyazied Abdallh, A.; Sergeant, P.; Dupré, L. Analysis and selection of harmonics sensitive to demagnetisation faults intended for condition monitoring of double rotor axial flux permanent magnet synchronous machines. *IET Electr. Power Appl.* **2018**, *12*, 486–493. [CrossRef]

25. De Bisschop, J.; Abdallh, A.; Sergeant, P.; Dupré, L. Identification of demagnetization faults in axial flux permanent magnet synchronous machines using an inverse problem coupled with an analytical model. *IEEE Trans. Magnet.* **2014**, *50*. [CrossRef]
26. Saavedra, H.; Riba, J.-R.; Romeral, L. Magnet shape influence on the performance of AFPMM with demagnetization. In Proceedings of the 2013 Annual Conference of the IEEE Industrial Electronics Society (IECON), Vienna, Austria, 10–13 November 2013.
27. Bahador, N.; Darabi, A.; Hasanabadi, H. Demagnetization analysis of axial flux permanent magnet motor under three phase short circuit fault. In Proceedings of the 2013 Annual International Power Electronics, Drive Systems and Technologies Conference, Tehran, Iran, 13–14 February 2013.
28. De Bisschop, J.; Vansompel, H.; Sergeant, P.; Dupré, L. Demagnetization Fault Detection in Axial Flux PM Machines by Using Sensing Coils and an Analytical Model. *IEEE Trans. Magnet.* **2017**, 53. [CrossRef]
29. Barmpatza, A.C.; Kappatou, J.C. Demagnetization Faults Detection in an Axial Flux Permanent Magnet Synchronous Generator. In Proceedings of the 2017 IEEE International Symposium on Diagnostics for Electrical Machines, Power Electronics and Drives (SDEMPED), Tinos, Greece, 29 August–1 September 2017.
30. Barmpatza, A.C.; Kappatou, J.C. Study of the Demagnetization Fault in an AFPM Machine in Relation with the Magnet Location. In Proceedings of the 2018 International Conference on Electrical Machines (ICEM), Alexandroupoli, Greece, 3–6 September 2018.
31. De Bisschop, J.; Sergeant, P.; Hemeida, A.; Vansompel, H.; Dupré, L. Analytical Model for Combined Study of Magnet Demagnetization and Eccentricity Defects in Axial Flux Permanent Magnet Synchronous Machines. *IEEE Trans. Magnet.* **2017**, 53. [CrossRef]
32. Kappatou, J.C.; Zalokostas, J.D.; Spyratos, D.A. 3-D FEM Analysis, Prototyping and Tests of an Axial Flux Permanent-Magnet Wind Generator. *Energies* **2017**, *10*, 1269. [CrossRef]
33. Radwan-Praglowska, N.; Wegiel, T.; Borkowski, D. Parameters Identification of Coreless Axial Flux Permanent Magnet Generator. *Arch. Electr. Eng.* **2018**, *62*, 391–402. [CrossRef]
34. Urresty, J.C.; Riba, J.-R.; Romeral, L. A Back-emf based method to detect magnet failures in PMSMs. *IEEE Trans. Magnet.* **2013**, *49*, 591–598. [CrossRef]
35. Urresty, J.C.; Riba, J.-R.; Romeral, L. Influence of the stator windings configuration in the currents and Zero-Sequence voltage harmonics in permanent magnet synchronous motors with demagnetization faults. *IEEE Trans. Magnet.* **2013**, *49*, 4885–4893. [CrossRef]
36. Goktas, T.; Zafarani, M.; Akin, B. Discernment of broken magnet and static eccentricity faults in permanent magnet synchronous motors. *IEEE Trans. Energy Convers.* **2016**, *31*, 578–587. [CrossRef]
37. Barmpatza, A.C.; Kappatou, J.C. Study of the Total Demagnetization Fault of an AFPM Wind Generator. *IEEE Trans. Energy Convers.* **2020**. [CrossRef]